Specially developed LR-0 reactor graphite environment for gen IV reactor support and cross-section measurement

Tomas Peltan[1, 2,*], Eva Vilimova[1], Tomas Czakoj[2], Zdenek Matej[3], Filip Mravec[3], Frantisek Cvachovec[3], Jan Simon[2], Vlastimil Juricek[2], Michal Kostal[2]

[1]University of West Bohemia in Pilsen, Czech Republic
[2]Research Centre Rez, Czech Republic
[3]Masaryk University in Brno, Czech Republic
(*) peltan@fel.zcu.cz

***Abstract*—This paper is focused on the development of the experimental environment connected to reactor graphite. Regarding its very good neutronic and mechanical properties, graphite will be very important in some new reactor designs, such as high-temperature or molten salt SMR reactors. These new reactor concepts require a new experimental environment as support for further research. In the laboratories of the Research Centre Řež and at the LR-0 reactor, the new experimentally validated graphite environment was created. This large graphite insertion is the largest graphite mono-block, which is possible to assemble at the LR-0 reactor. Sets of experiments for measuring reaction rates of different activation detectors for neutron field mapping were performed. This approach was used for thermal and epithermal region descriptions. For the fast neutron spectrum evaluation, the stilbene scintillation detector was used. All parameters, such as criticality height of moderator level, neutron spectrum, and other parameters for all experiments, were performed using Monte Carlo neutronic codes Serpent and MCNP. The obtained results were finally compared to the measurement of neutron leakage spectra from the graphite cube and graphite cylinder. These specially developed graphite-shaped neutron fields, reactor insertions, and external cube and cylinder with Cf neutron source can be used in the future for validation of not only materials used in SMR reactors but for arbitrary cross-section verification.**

***Keywords* — LR-0 reactor, a research reactor, graphite, cross-section, neutron leakage spectra, californium leakage spectrum**

I. Introduction

The reactor graphite has become a more popular material in Gen IV reactors. It can be used as a neutron reflector or a moderator in nuclear reactors due to very good neutron properties and mechanical behavior during irradiation and thermal stresses. Graphite is a very important material for a wide range of common nuclear reactor types such as Gas Cooled Reactors (GCR) and Light Water Graphite Reactors (LWGR) and even for newly developed reactors such as Molten Salt Reactors (MSR) or other currently very popular Small Modular Reactors (SMR).

Regarding the promising future of SMR reactors, a new adequate experimental environment and research facilities should be designed.

Although the behavior and neutron properties of the graphite are well known, there are still some discrepancies in graphite microscopic cross-section [1] , which can play a non-negligible role in new reactor development.

Moreover, currently worldwide is a lack of well-characterized neutron fields in graphite that can be used for experimental purposes. This article deals with a preliminary characterization of the graphite neutron field in a special large graphite insertion in the LR-0 experimental reactor. With the unique graphite insertion, the LR-0 reactor core could serve as a new reference neutron field for various experiments requiring a precise thermal and epithermal neutron spectrum.

This paper presents the results of a neutron distribution mapping performed using a set of activation foils selected according to their suitable microscopic cross-sections for thermal and epithermal neutron field reconstruction to characterize the neutron field of a large graphite prism. Then the paper analyses a fast neutron spectrum measured by the stilbene detector above 1 MeV and compares the experimental data from measurement in the LR 0 reactor with calculations performed in Monte Carlo code MCNP.

A. Experimental reactor LR-0

Reactor LR-0 is a zero power, light water pool type reactor located in the Research Centre Rez (Czechia). The LR-0 reactor was designed to research pressurized water reactor (PWR) physics (mainly for VVER-type cores). Its special design allows multi-purpose use. The technological equipment allows the carrying out of experiments on VVER-1000 or VVER-440 type assemblies.

The criticality of the reactor is reached by pumping a moderator to the reactor tank to the critical height, which is preliminarily calculated and latterly experimentally derived. As a moderator, pure demineralized water or a mixture of light water and boric acid up to 12 g/kg can be used. The second way how to reach criticality is by using control rods. The absorbing elements are boron carbide pellets in stainless-steel tubes.

Fuel assemblies are mockups of shortened VVER-1000

elements, which means a Zr cladding tube with an outer diameter of 9.15 mm filled with sintered UO_2 pellets. The active length of the fuel pin is 125 cm, and the total length is 135.7 cm. Other parameters are the same in the radial sense as the standard fuel assemblies VVER-1000. The characteristics of the reactor enable a wide range of experiments and different core arrangements.

Continuous nominal thermal power is 1 kW with thermal neutron flux ≈ 10^{13} m^{-2} s^{-1}. Fig. 1 shows the photo of the reactor core arrangement presented in this research.

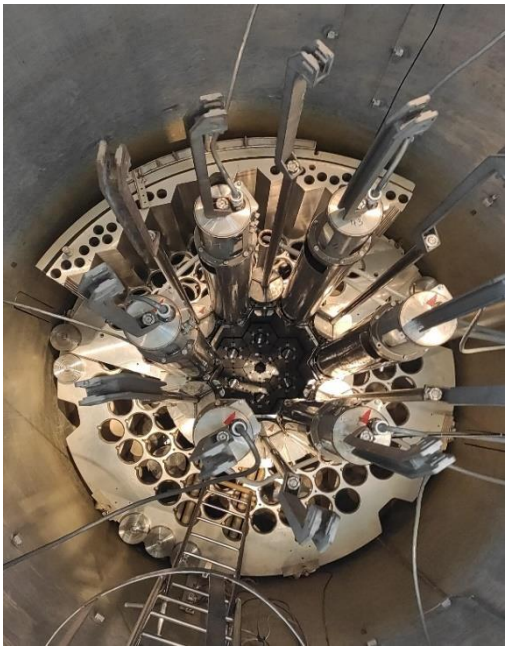

Fig. 1. LR-0 reactor core arrangement with central graphite insertion

II. Experimental and calculation methods

A. *Reactor core arrangement*

Twelve fuel assemblies surround a special dry experimental module, corresponding to seven fuel assemblies in size and shape. The dry experimental module is made of pure aluminum walls and assembled with stainless steel bottom weights and a support socket located in the lower part of the whole module. The dry module support socket fits to fuel construction supports of the reactor. The complex geometry of this special module allows the placement of the graphite blocks into the dry module in very tight geometry without significant air gaps, which keeps the module dry during all phases of the experiment. This feature, together with the addition of central graphite cylinder plugs, ensures a very “clean” neutron field dependent only on the embedded material because there is no additional excess structural material or water gaps between the separate experimental modules. The visualization of the reactor core, with developed large graphite insertion in the dry experimental module, can be seen in Fig. 2.

The experimental dry module is filled with seven identical graphite blocks. Each block consists of six smaller trapezoidal parts with a central cylinder in tight geometry. These seven blocks were installed on a special aluminum base for easier handling. The height of each graphite block is 60 cm with a hexagonal key dimension of 21.65 cm. The graphite insertion used in these experiments has a density of 1.72 ± 0.02 g/cm^3, a concentration of impurities below 0.2 ppm of boron equivalent. These properties meet the nuclear graphite limits [2] .

In this case, fuel assemblies have a nominal enrichment of 3.59 % and 3.60 % of ^{235}U. The fuel pins have a pin pitch of 1.275 cm, and fuel assemblies have a pitch formed of 23.6 cm, the same as in VVER-100 fuel geometry. The experimentally determined critical level of the moderator in the reactor was determined based on three independent measurements to H_{cr} = 39.133 ± 0.005 cm. Fuel assemblies are surrounded by nine dry aluminum installed 4 cm away from the core in a light water reflector. These channels serve for neutron monitoring regarding the reactor operation.

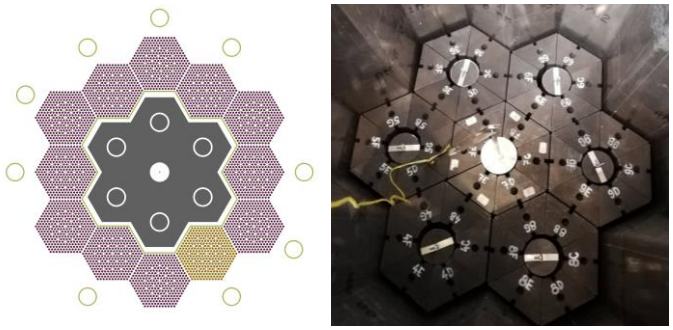

Fig. 2. Schematic view on reactor core arrangement (left), photo of real graphite insertion in the reactor core (right)

B. *Activation detectors and reactor core arrangement*

The specially developed activation foil holder is a single pure aluminum rod with a diameter of 0.8 cm and a special spatial displacer to ensure the precise position in the center of the graphite prism. Activation detectors were attached to this special holder. The distance between each activation material was manually set to 5 cm in the axial direction, which gives us seven axial positions in this case. This distance sufficiently ensures no neutron field disruption and interface effects between detectors. The Au, Cu, Fe, and Mn activation detectors were chosen for these purposes. The size of all activation detectors was 3 x 3x 0.1 mm. Only the manganese detector was spherical in diameter of less than 1 mm.

Irradiation of the activation foils was performed in two days irradiation, taking 9 hours each day to reach sufficient activity of detected radionuclides. Reactor power during irradiation was approximately 5 W.

C. *Graphite cube measurement with ^{252}Cf neutron source*

The measurement with a ^{252}Cf neutron source in a graphite cube geometry was performed at a special laboratory connected to the LR-0 facility [3] . The dimension of the whole laboratory is 5 x 5 x 7.2 m (height). The graphite cube was hung 2 m above the floor, which minimizes the neutron scattering from the wall and floor (the so-called room effect). The length of the edge of the graphite cube is 30 cm, and the cube is constructed from four smaller cubes tied together. In the center of the cube is a 2.5 cm diameter cavity for placing the flexo-rabbit system for

the neutron source movement.

The neutron leakage spectra were measured only by the stilbene detector for the purposes of this paper. The detector was placed 1 m away from the cube side, and the center of the crystal was set to the center of the neutron source in the central part of the cube. The graphite used in this experiment has a 1.72 g/cm^3 density, and the purity of this graphite is also very high.

This experiment was carried out by two independent measurements, one for fast neutron measurement, and the second with the special shielding cones. Measuring with the cones helps us evaluate the room effect and correct measured results regarding this measurement. The schematic diagram of the experiment can be found in Fig. 3.

Fig. 3. Measuring the neutron leakage spectra in special laboratory [3]

D. HPGe detector measurement and reaction rate determination

After the irradiation in the reactor core, the activity of irradiated activation detectors was measured using a well-defined HPGe coaxial vertical detector (Ortec GEM35). The HPGe detector efficiency was calculated using MCNP6 code in previous work, see [4] . The precise computational model for the detector was compiled using experimentally determined dimensions by a special radiogram of the crystal REF, and precisely measured dead layer. The efficiency curve of the used HPGe detector can be found in Fig. 4 compared to different models developed in the MCNP code.

Using the HPGe detector, the Net Peak Areas (NPA) of irradiated activation foils were measured. The calculations with a fixed source of neutron spectrum were used to determine the resonance self-shielding factors. Other necessary correction factors and parameters were obtained based on other MCNP calculations. The reaction rate of radioisotopes originating during non-constant irradiation power level in the reactor core is derived using Equations (1) and (2), while the capture reactions of the produced radioisotopes are neglected. Coincidence summing effect correction was calculated based on the method presented in previous work, see [7] .

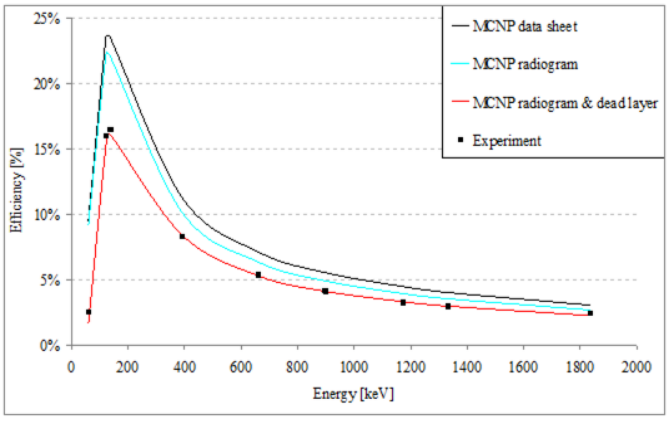

Fig. 4. Calculated and experimentally evaluated efficiency of the mentioned HPGe detector

$$the\ \frac{A(\underline{P})}{A_{Sat}(\underline{P})} = \sum P_{rel}^{i} \times \left(1 - e^{-\lambda.T_{Ir}^{i}}\right) \times e^{-\lambda.T_{end}^{i}} \quad (1)$$

$$q(\underline{P}) = \left(\frac{A(\underline{P})}{A_{Sat}(\underline{P})}\right)^{-1} \times NPA(T_M) \times \frac{\lambda}{\varepsilon \times \eta \times N} \times \frac{\frac{t_{real}}{t_{live}}}{(1 - e^{-\lambda.T_m})} \times \frac{1}{e^{-\lambda.\Delta T}} \times \frac{1}{k_{CSEF}} \times k_{SSEF} \quad (2)$$

where:

$\frac{A(\underline{P})}{A_{Sat}(\underline{P})}$ is relative portion of saturated activity induced during irradiation experiment,

P_{rel}^{i} is relative power on the i-th day of irradiation, $P_{rel}^{i} = \frac{P^{i}}{\underline{P}}$,

$q(\underline{P})$ is reaction rate of activation foil during power density $\underline{P}$,

T_{ir}^{i} is irradiation time on the i-th day of irradiation,

T_{end}^{i} is time from the end of i-th day of irradiation to end of all irradiations,

λ is the decay constant of corresponding material,

T_m is the time of activation foil measurement by HPGe,

ΔT is the time between the end of irradiation and the start of HPGe measurement,

$NPA(T_m)$ is the measured number of counts,

ε is gamma branching ratio of activation material – depending on the material,

η is detector efficiency – the result of MCNP calculation,

N is number of target isotope nuclei in activation foil,

t_{real} is the real-time of counting system of the HPGe (= T_m),

t_{live} is the live time of the counting system of the HPGe ($< t_{real}$),

k_{CSEF} is the coincidence summing effect correction,

k_{SSEF} is the resonance self-shielding effect correction determined by MCNP.

E. Stilbene detector measurement

The neutron flux up to 1 MeV was measured with a two-parameter multichannel analyzer, which is fully digitized, and can process up to 300 000 impulses per second [8] . The input analog signal from the photomultiplier is divided in the preamplifier into two branches. Each branch is differently

amplified in ratio 1:8 and digitized by separate A/D converts with 12 bits resolution. The stilbene scintillator of cylindrical geometry with dimensions ø 10 mm × 10 mm coupled to the photomultiplier RCA 8575 was used as the neutron detector. Since stilbene is an organic scintillation detector, it is sensitive not only to neutrons but also to gamma. The separation between neutron and gamma pulses is realized by means of pulse shape discrimination (PSD) of the measured response. Pulse Shape Discrimination parameter (D) is derived by an integration algorithm, which principle lies in the comparison of area limited by part of a trailing edge of the measured response (*Q1*) with area limited by the whole response (*Q2*). The areas *Q1* and *Q2*, as integrals over time, are expressed in Equation (3), and their illustration is shown in Fig. 5.

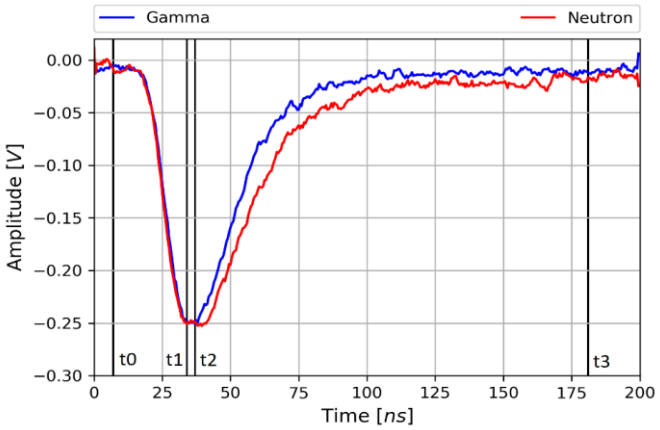

Fig. 5. Comparison of real neutron and gamma pulses from Stilbene scintillation detector with marked examples of a separation boundary for integration algorithm

The time offset t_2 is set for the optimal discrimination properties (namely, the most significant possible difference in the discrimination parameter for neutrons and gammas) to about 1/10 to 1/3 of the trailing edge. This parameter is different regarding the scintillation detector type.

Charge Q_1 is determined by an area limited by the response course within a time interval (t_2, t_3). The charge Q_2 is determined by an area limited by the response course within firmly defined times t_0 and t_3. Times t_0 and t_3 depend on the parameters of the measuring apparatus, and time t_3 is defined as the end of the response.

Using PSD, energy-dependent recoil proton responses $S(E_p)$ are evaluated. The neutron fluxes are then evaluated by deconvolution according to Equation (4). The response matrix of the crystal $K(E_N, E_P)$ was determined employing Monte Carlo code NEU-7 [9] [10] [11] .

$$Q_1 = \int_{t_2}^{t_3} i(t)dt, \quad Q_2 = \int_{t_0}^{t_3} i(t)dt, \quad D = \frac{Q_1}{Q_2} \tag{3}$$

$$S(E_p) = \int K(E_N, E_P)\phi(E_N)dE_N \tag{4}$$

The stilbene detector is very suitable for measuring higher neutron energies. The ability to accurately measure stilbene at energies above 1 MeV was demonstrated by a specially designed experiment on the LVR-15 reactor. The neutron beam in one radial port was filtered by a 100 cm thick plug of high-purity silicon monocrystals. This filter appropriately shapes the neutron spectrum, making it possible to accurately calibrate the apparatus [12] . The comparison between simulation and real measurement can be found in Fig. 6

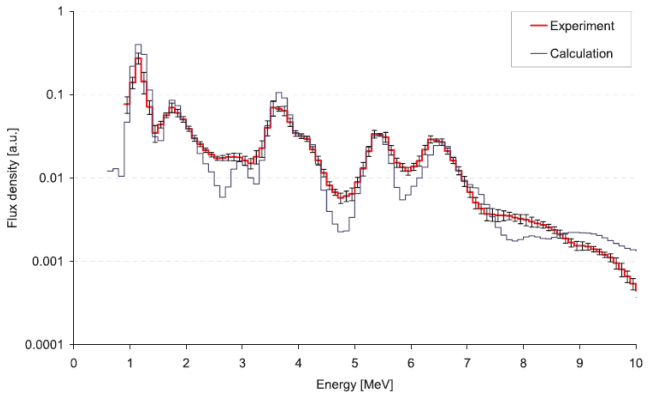

Fig. 6. Calculated and experimentally measured neutron flux on Si filtered neutron beam with stilbene detector [12]

Stilbene was used to measure the neutron leakage spectrum in the range of 1 MeV to 10 MeV in the group structure with energy steps of 100 keV. The total uncertainty of measurement in both experiments was estimated between 1.9% and 10.5%, depending on energy and position in the experiment.

F. Calculations

Reactor experiment

The neutron transport and neutron spectra simulations were carried out using the MCNP 6.2 [13] Monte Carlo code with ENDF/B-VII.1 [14] nuclear data library and corresponding TSL (Thermal Scattering Library). The whole reactor core was modeled in accurate dimensions and shapes, the only simplification being the neglect of a small air gap in each graphite block. The simplification was done by homogenizing the air cavity and graphite blocks by changing the density of the whole graphite module to ensure the same amount of graphite in each module and reactor core.

Neutron spectra were calculated in each seven axial positions in the activation foil holder. The calculation was performed at a fixed critical level of the moderator obtained experimentally, critical height was set to H_{cr} = 39.133 cm. The number of simulated neutrons was 40,000 neutrons per cycle in 585,000 active cycles with 50 inactive cycles. The statistical uncertainty of the calculated neutron spectrum, reached in the central position 3 of the holder, is below 2% in each energy group in the energy range from 1×10^{-8} MeV to 3 MeV. In higher and lower energy regions, the statistical uncertainty in each energy group slightly rises. Obtained neutron spectrum serves as a defined neutron spectrum for reaction rate calculation in activation materials described in the sections above.

Reaction rates of all activation foils were calculated separately with a fixed neutron spectrum source and the exact shape of the activation detector in the separate MCNP

calculation. In each calculation step, 1×10^9 source neutrons were simulated with an energy spectrum corresponding to the precise position in the activation foil holder. The statistical uncertainty in the calculated reaction rate was between 0.3% and 0.7%, depending on the activation material and size. Finally, the correction factors and self-shielding factors were calculated for all positions and all materials.

Reaction rates of all foils used for neutron mapping in the activation foil holder and comparison with the experiment were manually calculated using the scalar multiplication of the calculated neutron spectrum in a defined position and microscopic cross-section obtained from ENDF/B-VIII.0 [15] nuclear data library. This technique determines the reaction rate per atom in each activation foil.

MCNP was also used to calculate a wide range of the neutron spectrum. The ENDF/B-VIII.0 nuclear data library was used with a corresponding TSL matrix with 30% graphite porosity, consistent with previous research on graphite calculations and experiments performed on the LR-0 reactor. The calculation was carried out with 200,000 neutrons per cycle in 20,000 active and 50 inactive cycles. The detection volume was the same size and position as a stilbene detector volume placed in the center of the height of the moderator level. The uncertainty of the calculated neutron spectrum is below 0.8% in energy ranges from 1×10^{-8} MeV to 3 MeV.

Graphite cube experiment.

As in the previous section, the MCNP Monte Carlo code with ENDF/B-VII.1 nuclear data library was used to calculate the neutron leakage spectrum from the graphite cube. In this case, Mannhart's [16] neutron spectrum for ^{252}Cf simulation was used. As graphite, the same composition as in the reactor experiment was used. The energy grid structure of the simulated detector was set to the same energy resolution as in the stilbene measurement.

III. Results

A. Reaction rate measurement in LR-0 graphite core

Regarding the methodology described above, the activity of the activation detectors was measured on the HPGe detector and then calculated based on Equations (1) and (2). Estimated reaction rates based on measurement were normalized using a scaling factor. The scaling factor is a calculated constant representing the neutron emission in the reactor core. For the scaling factor calculation, the average calculated values based on Ta and $_{1\%}$Au activation foils were used (axial positions 2, 3, and 4 in the activation foil holder). The Ta and $_{1\%}$Au were used only like a power monitor during irradiation, and the reaction rate of these foils is not a part of this work. After that, the scaling factor was multiplied by the self-shielding correction factor and divided by the calculated reaction rate from the MCNP calculation. The results of all mentioned calculations lead to the experimentally determined scaling factor to be 4.245×10^{11} with 0.86% statistical uncertainty. The thermal power of the reactor during irradiation can be estimated based on the number of neutrons per fission, 2.447 neutrons, with fission energy released of 180.9034 MeV. All these parameters were obtained from the MCNP output file. From these values, the irradiation power was calculated to be approximately 5 W.

Table I shows experimentally determined reaction rates of the selected activation foils. The statistical uncertainty of measurement has been quantified with a combination of measured geometry uncertainty and uncertainty of HPGe detector below 0.79 % for all observed activation detectors.

Table I
Experimentally determined reaction rates of activation foil per one atom in the exact axial position on the foil holder - central rod. The unit [1/s]

Pos.	Au	Cu	Fe	Mn
1	7.650E-27	1.872E-28	5.406E-29	5.311E-28
2	8.441E-27	2.040E-28	5.990E-29	5.733E-28
3	9.171E-27	2.047E-28	5.996E-29	6.122E-28
4	9.489E-27	2.083E-28	5.866E-29	6.290E-28
5	8.990E-27	2.005E-28	-	6.077E-28
6	8.896E-27	1.912E-28	5.167E-29	5.511E-28
7	7.877E-27	1.698E-28	4.664E-29	4.830E-28

For a better comparison of obtained experimentally determined results with MCNP calculation, the C/E-1 (calculation/experiment-1) ratio was estimated, see Table II.

Table II
Calculated C/E-1 for presented activation detectors

Pos.	Au	Cu	Fe	Mn
1	-0.01%	-9.64%	-8.88%	-5.22%
2	5.49%	-4.88%	-5.87%	-0.05%
3	5.24%	0.10%	-0.86%	-1.01%
4	1.31%	-2.68%	0.57%	-4.41%
5	0.85%	-6.07%	-	-7.90%
6	-10.58%	-13.98%	-7.45%	-11.55%
7	-17.03%	-21.08%	-16.61%	-18.04%

An excellent agreement between measurement and calculation can be observed in positions 3 and 4, position 5 is sometimes better no, which is caused by its position in the axial center of the activation holder. Position 5 is close to the spacing grid of fuel, which can slightly affect the measured results. In contrast, positions 1, 2, and 6, 7 are underestimated for almost all detectors. Position 1 and 2 are placed in the bottom part of the holder, which caused inhomogeneity in the neutron field caused by construction parts of a special experimental channel where the graphite prism is placed. Under the channel, the stainless-steel weight and more water below the fuel can be found, which can negatively affect the neutron flux by these materials, which seems like heavy reflector with shifted neutron spectrum. At the same time, other boundary phenomena, such as the end of the fuel column in this area, may play a non-negligible role in neutron spectra shaping.

The situation is slightly different on the other side of the foil holder. Position 6 is in the axial position, corresponding to the moderator-air interface. Position 7 is placed above the moderator water level but still in graphite blocks. Position 7 shows the highest inconsistency of all detectors examined. As the difference between the moderator level and the position of

the activation foil increases, the underestimation rises. This phenomenon was previously observed and described in different type of experiment with a partially flooded reactor core, see [17] .

The central positions are the most suitable for future cross-section testing or for another irradiation experiment, which means axial positions 3, 4, and 5. In these positions, the neutron flux is the most homogeneous. The precise positioning will depend on the material properties, size, and the requirement for the shape of the neutron spectrum.

B. Fast neutron spectra measurement in LR-0 graphite core

In this step, the main goal was to evaluate the neutron spectrum in the fast energy region. Activation detectors presented in this work are sensitive only in thermal and epithermal energy regions, so the stilbene was chosen for fast neutron mapping.

Mapping the fast neutron flux using activation detectors case appears to be very complicated because a minimal amount of the fast neutrons reaches this central well-moderated position. The second issue is that the threshold reactions commonly used for these purposes have a small cross-section, which complicates the measurement.

The preliminary assumption about the well-thermalized neutron spectrum has been verified based on activation detector measurement and MCNP calculation. For better imagination of the graphite shaping influence, the three different reactor core neutron spectrum calculation by MCNP is shown in Fig. 7.

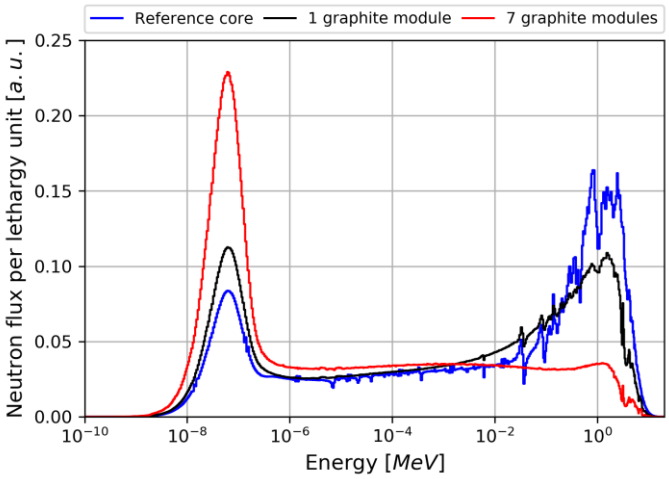

Fig. 7. Calculated neutron spectrum for reference core (blue curve), one graphite module in the centre of the reference core (black curve) and proposed seven graphite reactor core (red curve)

In contrast to the reference LR-0 core [18] , the red curve shows significant thermalization occurring in the proposed reactor core with a thermal neutron ratio of almost 25% and a fast neutron ratio of less than 4% above 1 MeV. It can be noticed that a small amount of graphite (case with only one block in the center of the reference core) slightly increases the number of thermal neutrons in the detector position but hardly decrease the number of fast neutrons, see the comparison of blue and black curve. The epithermal region in large graphite case is nearly constant, which can be helpful for cross-section evaluation.

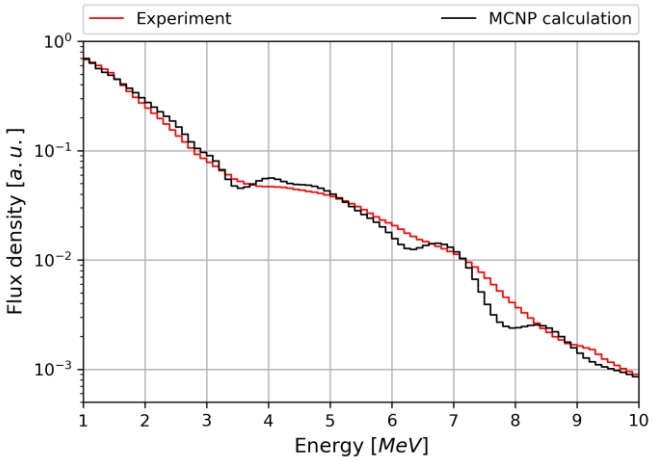

Fig. 8. Comparison of the experimentally measured fast neutron spectrum by stilbene detector and spectrum calculated by MCNP code – LR-0 reactor experiment

The last part of the modeled neutron spectrum from Fig. 7 was compared with the real measurement provided by the stilbene detector. The measurement was carried out from 1 MeV to 10 MeV. For this purpose, the calculated and measured spectrum was normalized to 1 in the range from 4 MeV to 10 MeV. This normalization is advantageous due to ensure that the gamma counts do not contribute to neutron spectra. The calculation was finally modified by the Gaussian broadening function based on experimentally determined parameters for stilbene detector. The comparison between calculation and measurement can be seen in Fig. 8.

Due to the resolution and measured energy grid structure of the stilbene crystal, the sharp resonances cannot be recognized. The agreement between calculation and measurement is very well in the range from 1 MeV to 5.8 MeV. With increasing energy of the neutrons, the deviation starts rising except for 7 MeV. Maximal disagreement can be observed around the 7.8 MeV.

C. Fast neutron leakage spectra measurement with graphite cube and ^{252}Cf neutron source

The fast neutron leakage spectrum was measured with a ^{252}Cf neutron source. Using the californium neutron source instead of ^{235}U and comparing them to each other is legit because the ^{252}Cf neutron source is often mentioned as the neutron PFNS standard [3] . The differences between uranium and californium are very small, so they can be compared without any complications.

The results from the measurement on the graphite cube compared to the calculation in MCNP code can be found in Fig. 9. The comparison of measurement and MCNP calculation provides the same trend in neutron spectra shape [19] . Up to 6.5 MeV, the agreement between measurement and experiment is perfect. Only one problematic region, slightly similar behavior as in Fig. 8, was observed between 3.1 MeV and 4 MeV. In this case, probably the resolution of the stilbene detector plays the main role. In graphite cross-section, a very sharp resonance exists in this area, which can cause the deformation of a few surrounding energy bins. In higher energies up to 6.5 MeV, the discrepancy between measurement and calculation rises. In energies up to 9 MeV, the agreement is again perfect.

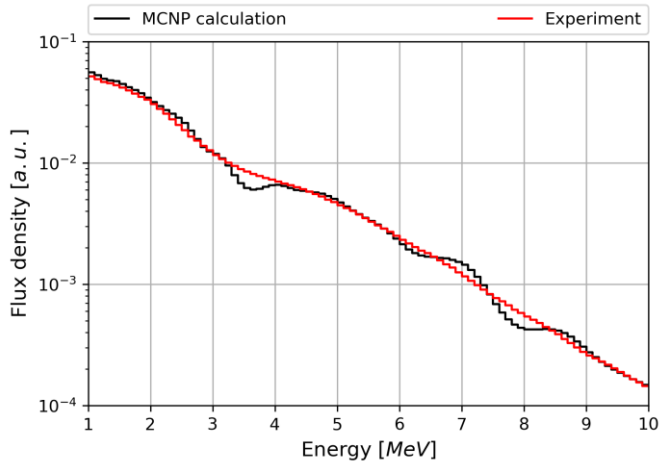

Fig. 9. Comparison of the experimentally measured fast neutron spectrum by stilbene detector and spectrum calculated by MCNP code – graphite cube with ^{252}Cf neutron source

For better imagination and better comparison between both experiments and the calculated results, the C/E-1 (calculation/experiment-1) chart shows the behavior of this phenomena in one chart, see Fig. 10.

It can be noticed that even if the experimental setup of the graphite cube is quite different compared to the LR-0 core, the same trends in the behavior of the fast neutrons neutron spectra shape can be observed in Fig. 8 and Fig. 9.

In the LR-0 experiment setup, the neutrons go from outside to the middle of the graphite geometry. In the case of the graphite cube, the neutrons transport oppositely from the source in the center to the outside.

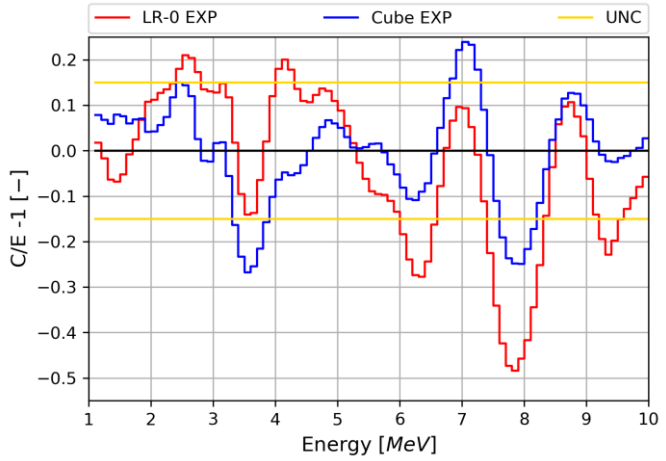

Fig. 10. Comparison of both experiments in C/E-1 methodology

In Fig. 10, the same behavior explained in the upper section is more evident. The yellow lines serve to imagine the maximal possible uncertainty caused by the methodology of the experiment and stilbene measurement. One can notice that in both cases, the most problematic energetic region is from 6 MeV to 8.5 MeV. This effect is probably multiplied by the amount of filtering graphite. With the increasing amount of graphite in the experiment, the energies higher than 6 MeV are in much worse agreement than the cube and the LR-0 experiment. The amount of graphite and the different behavior of neutron flux was previously observed and investigated in [20] [21] [22] .

More significant disagreement in both experiments is located around 7.8 MeV.

IV. Conclusions

In this work, a comparison of two independent experiments with rector graphite was performed. The first experiment in the LR-0 core provides very good results in thermal and epithermal energies. Another benefit is the fact that graphite filter effectively decreases the number of fast neutrons to a very low share. The epithermal region is almost flat and approx. 25% of all neutrons are in thermal energy. This core configuration can be used in the future for various types of experiments regarding validation of the cross-section in thermal and epithermal energies with a cadmium filter, for example.

On the other hand, the fast neutron spectrum filtered by graphite shows some deficiencies in the description of graphite nuclear data. The biggest discrepancy between measurement and calculation was observed in the energy region from 6 MeV to 9.5 MeV. This discrepancy may be caused by inaccuracy in the graphite cross-section around the 6-8 MeV energy region, probably a combination of the elastic and inelastic cross-section.

Finally, these results lead to the development of new reactor core arrangements with a special arrangement of graphite block to confirm or refute the finding mentioned higher in this work.

ACKNOWLEDGEMENT

The presented results were obtained using the CICRR infrastructure, which is financially supported by the Ministry of Education, Youth and Sports – project number LM2023041, supported by Energy Storage TK02030069 project and special project SGS-2021-018.

References

[1] Brown, D.A. ‘ENDF/B-VIII.0: The 8th major release of the ENDF/B library containing Cielo-project evaluations, new standards and thermal scattering data’, 20th Topical Meeting of the Radiation Protection and Shielding Division, RPSD 2018, 148, pp. 1–142

[2] Bolewski, A. et al. ‘A practical method for measuring the boron equivalent of graphite impurity’, Nuclear Instruments and Methods in Physics Research, Section B: Beam Interactions with Materials and Atoms, 237 (3–4), 2005 pp. 602–612. Available at: https://doi.org/10.1016/j.nimb.2005.03.002

[3] Schulc M. et al. ‘Application of ^{252}Cf neutron source for precise nuclear data experiments‘, Applied Radiation and Isotopes, 2019,Vol 151, 187-195, Available at: https://doi.org/10.1016/j.apradiso.2019.06.012

[4] Košťál, M. et al. ‘Measurement of various monitors reaction rate in a special core at LR-0 reactor’, Annals of Nuclear Energy, 112, 2018, pp. 759–768. Available at: https://doi.org/10.1016/j.anucene.2017.10.036

[5] Dryak, P. and Kovar, P. ‘Experimental and MC determination of HPGe detector efficiency in the 40-2754 keV energy range for measuring point source geometry with the source-to-detector distance of 25 cm’, Applied Radiation and Isotopes, 64(10–11), 2006, pp. 1346–1349. Available at: https://doi.org/10.1016/j.apradiso.2006.02.083.

[6] Boson, J., Ågren, G. and Johansson, L. ‘A detailed investigation of HPGe detector response for improved Monte Carlo efficiency calculations’, Nuclear Instruments and Methods in Physics Research, Section A: Accelerators, Spectrometers, Detectors, and Associated Equipment, 587 (2–3), 2008, pp. 304–314. Available at: https://doi.org/10.1016/j.nima.2008.01.062

[7] Tomarchio, E. and Rizzo, S. 'Coincidence-summing correction equations in gamma-ray spectrometry with p-type HPGedetectors', Radiation Physics and Chemistry, 80(3), 2011, pp. 318–323. Available at: https://doi.org/10.1016/j.radphyschem.2010.09.014.
[8] Veskrna et al. 'Digitalized two parametric system for gamma/neutron spectrometry' 18th Topical Meeting of the Radiation Protection & Shielding Division of ANS, Knoxville, TN USA, 2014.
[9] Bureš, Z. et al. 'Multiparameter Multichannel Analyser System for Characterisation of Mixed Neutron – Gamma Field in the Experimental Reactor Lr-O', in Reactor Dosimetry in the 21st Century: Proceedings of the 11th International Symposium on Reactor Dosimetry Brussels, 2003, pp. 194–201. Available at: https://doi.org/10.1142/9789812705563_0025
[10] Cvachovec, J. et al. 'Neutron response function for BC-523A scintillation detector in the energy range 0.5 MeV to 20 MeV', Journal of ASTM International, 5(5), 2008. Available at: https://doi.org/10.1520/JAI101149.
[11] Veškrna, M. et al. 'Digitalized two parametric system for gamma/neutron spectrometry', in 18th Topical Meeting of the Radiation Protection and Shielding Division of ANS, RPSD, 2014. Knoxville, TN USA, pp. 216–219.
[12] Košťál M. et al. 'Measurement of neutron spectra in a silicon filtered neutron beam using stilbene detector at the LVR-15 research reactor', Applied Radiation and Isotopes 128, 2017, 41-48, Available at: https://doi.org/10.1016/j.apradiso.2017.06.026
[13] Werner, C.J. 'MCNP6TM User's Manual - Code Version 6.2'. Los Alamos: Los Alamos National Laboratory, 2017.
[14] Chadwick, M.B. et al. 'ENDF/B-VII.1 nuclear data for science and technology: Cross sections, covariances, fission product yields and decay data', Nuclear Data Sheets, 112(12), 2011, pp. 2887–2996. Available at: https://doi.org/10.1016/j.nds.2011.11.002
[15] Brown, D.A. 'ENDF/B-VIII.0: The 8th major release of the ENDF/B library containing Cielo-project evaluations, new standards and thermal scattering data', 20th Topical Meeting of the Radiation Protection and Shielding Division, RPSD, 2018, 148, pp. 1–142.
[16] Capote, R. et al. 'Updating and Extending the IRDF-2002 Dosimetry Library' Journal of ASTM International, Vol. 9, No. 4, 2012, pp. 1-9, https://doi.org/10.1520/JAI104119. ISSN 1546-962X
[17] Košťál, M., Švadlenková, M., et al. 'Determining the axial power profile of partly flooded fuel in a compact core assembled in reactor LR-0', Annals of Nuclear Energy, 90, 2016, pp. 450–458. Available at: https://doi.org/10.1016/j.anucene.2015.12.028.
[18] Košťál, M. et al. 'A reference neutron field for measurement of spectrum averaged cross sections', Annals of Nuclear Energy, 2020, 140. Available at: https://doi.org/10.1016/j.anucene.2019.107119.
[19] Peltan, T. et al. 'Validation of graphite cross section in various integral experiments', in International Conference on Nuclear Engineering, Proceedings, ICONE, 2019. Available at: https://doi.org/10.1299/jsmeicone.2019.27.2083.
[20] Czakoj, T., Losa, E. and Košťál, M. 'Design of a special core for large graphite insertion studies in the LR-0 reactor', in PHYTRA4 – The Fourth International Conference on Physics and Technology of Reactors and Applications. Marrakesh, Morocco, 2018, pp. 238–249
[21] Vilímová E., et al. 'Position evaluation of ex-core neutron flux measurement in new type graphite reactors', The European Physical Journal Conferences, 2021, vol 253, Available at: ttps://doi.org/10.1051/epjconf/202125305005
[22] Košťál, M., Rypar, V., et al. 'Study of graphite reactivity worth on well-defined cores assembled on LR-0 reactor', Annals of Nuclear Energy, 87, 2016, pp. 601–611. Available at: https://doi.org/10.1016/j.anucene.2015.10.010.